Prospects of Phobos sample return mission using electrostatic container

Vladimir S. Aslanov[1]
Samara National Research University, 34, Moscovskoe shosse, Samara 443086, Russia

This paper explores the feasibility and benefits of a new way of the Phobos sample return delivery mission to a Phobos Sample Return (PSR) orbiter using the electrostatic field artificially generated in proximity to the Mars-Phobos L1 libration point. The proposed method utilizes the electrostatic interaction to retrieve an Orbit Sample container (OS) launched from Phobos. This is possibly the first discussion of the mission to deliver Phobos samples to a small area around a PSR orbiter for the subsequent capture of the OS, e.g., utilizing a magnetic trap or net. The feasibility of the proposed retrieval system is discussed from the aspect of local space weather Debye length. The container's motion is studied, and the conditions of reaching the small given vicinity, the L1 point, are determined. The proposed mission's principal feasibility is demonstrated. The influence of the electrostatic charge level and the Debye length is studied on the container trajectory and the possibility of capturing the container. In addition, the possible launching points of the container from the Phobos surface and the launching velocity at which the PSR orbiter can capture the container are determined by the backward numerical integration method of the motion equations.

Nomenclature

d = distance between Mars and Phobos, m

G = Newtonian gravitational constant, $6.67428 \cdot 10^{-11}$, $\mathrm{m}^3 \cdot s^{-2} \cdot kg^{-1}$

k_C = Coulomb's constant, $8.99 \cdot 10^9$ $N \cdot \mathrm{m}^2 / C^2$

m_1 = mass of Mars, kg

m_2 = mass of Phobos, kg

m_3 = mass of the container, kg

---

[1] Head of Department, Professor, Theoretical Mechanics Department, 34, Moscovskoe Shosse, aslanov_ vs@mail.ru

n = mean orbital rate of the space tug, rad / s

q_i = charge ($i = 2$ equal for the PSR orbiter and $i = 3$ for the container), C

x_{L_1} = abscissa of the Mars-Phobos L1 point, m

λ_D = Debye length, m

μ = $m_2 / (m_1 + m_2)$

Φ = product $k_C q_2 q_3$, $\mathrm{N \cdot m^2}$

Subscripts

1 = Mars

2 = Phobos

3 = Container

I. Introduction

Scientific missions to explore Mars and the Martian moon, Phobos, are of scientific interest because of their unknown origin and formation [1-9]. Returning samples from a planet provide an opportunity for new insights related to the planet's formation and configuration. In recent years, aerospace scientists looked at Martian sample return missions [1]. To get samples by landing the large return vehicle requires a large fuel requirement to offset the planet's gravity. In the Martian sample return missions, it has been proposed that an Orbit Sample container (OS) is launched using a Mars Ascent Vehicle after samples are collected by the Mars 2020 rover [8]. However, rendezvous and docking of an orbiter to catch the OS is a challenging and unsolved aspect of the current mission architecture. Also, rendezvous and docking in deep-space require autonomous navigation and control capabilities. An Earth-based ground station in real-time cannot control a deep-space satellite. As a solution to this deep-space docking challenge, the prospects of the OS utilizing electrostatic force has been discussed in [1]. In this paper, the proposed method utilizes the electrostatic interaction to retrieve the OS launched from a planet by a small rocket. To perform rendezvous and docking safely in orbit, the possibility of rotational motion control for a cylindrical OS was discussed. Observed that the sample container can not be launched to high orbit from Martian ground because a small launcher is used, hence there are some limitations to the operation of the proposed system to get the OS automatically using the Coulomb force. Operation of system using Coulomb force at a low altitude should be conducted with the short effective Debye length. Consequently, it is required that an orbiter approaches the OS to get within the range of the effective Debye length. In addition, high power is required to change the potential of the OS and the orbiter itself, which are limited. It is also shown in [1] that the proposed sample container retriever can suppress the attitude and angular velocity of the cylindrical OS under certain constraints related to the power that can be generated by generated by Solar Array Panel.

Let us consider the possibility of the approach based on the electrostatic interaction [1] as applied to Phobos. The Phobos exploration is of independent importance. Phobos sample return missions can be conducted to investigate Phobos and improve our understanding of the planets. In addition, Mars's moon, Phobos, can be positioned to support martian surface operations as a staging point for future human exploration. Phobos is a small, irregularly-shaped moon (~26 × 22.8 × 18.1 km) that orbits Mars every 7 hours and 39 minutes. The orbit is synchronous to its rotation so that its long axis is always directed toward Mars. The Mars-Phobos L1 libration point is unusually close to Phobos' surface (~ 3.4 km) due to its weak gravity and proximity to Mars. Note that the Mars-Phobos L1 location is not a fixed-point relative to the moon's surface. Since Phobos' orbit is slightly elliptical (9234.42 km x 9517.58 km), this causes the L1 location to have a periodic motion of a few hundred meters, relative to the moon's surface during each orbit. The average gravity for Phobos is commonly listed as 0.0057 m/s² [9]. This is a very low gravitational acceleration compared to Mars' gravity (3.5-3.7 m/s²). It is important to note the Russian Phobos-Soil [10, 11], which after the launch on November 8, 2011, crashed into the Pacific Ocean two months later. This mission should have included the landing of a heavy spacecraft (1270 kg) on Phobos, and the launch of a return vehicle (287 kg) from Phobos.

Low gravity acceleration, relatively small periodic deviations of the L1 point from the fixed position and proximity to Phobos surface make the container delivery mission to a Phobos Sample Return (PSR) orbiter technically and economically feasible if the PSR orbiter hovered near the Mars-Phobos L1 point. However, we must account for the L1 point having unstable orbital locations: once the PSR orbiter drifts away from these locations, it will not return. The PSR orbiter must actively maintain its position to remain near these locations. The more accurately it can maintain its position, the less fuel it will need to stay there. In the Phobos sample return missions, it can be proposed that an Orbit Sample container is launched by a launch platform or a Phobos rover after samples are collected. After launching the OS to the PSR orbiter that takes it back to the Earth and jettisons the OS protected by an Earth re-entry capsule. Note that in order to implement the proposed Phobos Sample mission, the Debye length λ_D should be considered. The Debye length is an important parameter because the Electrostatic field (E-field) rapidly decreases beyond this length by the Debye shielding effect. However, the Debye length near the L1 point is unknown; approximate Debye length values are given for the Stickney crater, located on Phobos' surface directly under the L1 point. Depending on Mars local time, this parameter ranges from 13 m to 47 m [12]. In the absence of accurate data, all calculations are performed for two values of this parameter 15 m and 45 m.

This paper aims to explore the feasibility and benefits of the proposed concept of the Phobos sample return delivery mission to the PSR orbiter using the electrostatic field artificially generated in proximity to the Mars-Phobos L1 libration point. The proposed mission implies that the PSR orbiter is at the L1 point and creates the E-field, the electrostatic Orbit Sample container will be launched from Phobos to the L1 point. The following stages of the mission: a capture of the OS, e.g., utilizing a magnetic trap [13] or net [14], when the OS reaches in the small vicinity of the orbiter, called a Capture Sphere. Contact capture of the container and its delivery to Earth using the PSR orbiter is not considered in this paper. The current work presents perhaps the first discussion on the Phobos sample delivery mission to the PSR orbiter.

The paper consists of six sections and a conclusion. In Section 1 (Introduction), the research objective is formulated. In section 2, the container delivery method concept to the Mars-Phobos L1 libration point is discussed in detail. In section 3, all key assumptions are given, the planar motion equations of the container relative to the L1 point are developed, and a new Jacobi integral is obtained, taking into account the E-field in analytical form for the restricted problem of three bodies. Section 4 studies the container's motion in the electrostatic field and determines the conditions of reaching the given small neighborhood of the L1 point using a backward numerical integration method of the motion equations. Numerical-analytical modeling is performed in Section 5 to substantiate the mission and select its main parameters. Lastly, the conclusions, together with the discussion, are presented in Section 6 (Conclusions).

II. Formulation of the problem

This paper aims to show the possibility of implementing the mission to deliver the sample from Phobos to a required small PSR orbiter vicinity. The mission should be relatively simple. The container is started by a simple starter device with a given velocity to be determined below. The PSR orbiter is proposed to be located in the Mars-Phobos libration point L1, which always looks toward Mars and is 3.4 km from the Phobos surface. Take into account that the L1 point is unstable, and the orbiter can remain at this point at the cost of the engines, the more accurately it can maintain its position, the less fuel it will need to stay there. However, the container as a third small body in the gravitational fields of Mars and Phobos without propulsion will not reach the L1 point because of its instability. This point's stability can be achieved by artificially attracting a potential electrostatic field owing to electrostatic charges of differing orbiter and container signs. The E-field's action is limited to the Debye sphere, a radius of the Debye length. The generation of electrostatic potential in the L1 leads to the previously unstable L1 point splitting to two unstable L6 and L7 points within the Debye, as illustrated in Fig. 1. When the electrostatic potential decreases, these points approach the L1 point, and when this potential disappears, the L6 and L7 points merge into one L1 point. The L6 and L7 libration points will be determined later. The configuration of other the Mars-Phobos libration points (L2, L3, L4 and L5) remains unchanged due to the E-field's limited action. Note also the E-field's appearance in the L1 point generates a new case of the restricted three-body problem in two gravity fields and one electrostatic field when there are six equilibrium positions (L2, L3, L4, L5, L6 and L7).

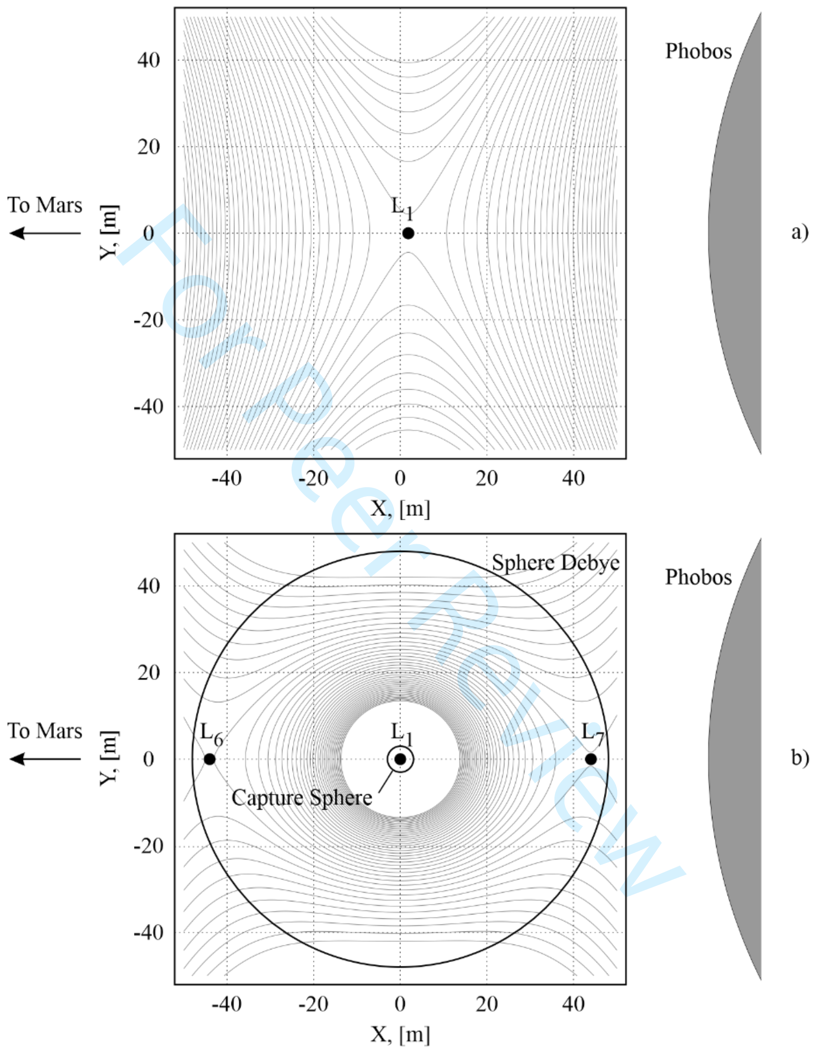

Fig. 1 Splitting of the unstable Mars-Phobos L1 libration point to two unstable L6 and L7 points (a – without E-field, b – with E-field)

The local mission's purpose is to reach the Capture Sphere in which the PSR orbiter is located (Fig. 1). Obviously, for convenient container capture, the container’s velocity - at the boundary of the Capture Sphere - should be as low as possible. On the other hand, not every container trajectory crossing the Debye Sphere reaches the Capture Sphere. A Hill Sphere, which in this case defines the area where the attraction center (the L1 point) for the electrostatic container dominates, is located inside the Debye Sphere. This area will be called the E-Hill Sphere.

The outer shell of that region constitutes a zero-velocity surface. In terms of the restricted three-body problem [15-18], the total energy is equal to the potential energy in the L6 and L7 saddles. It follows that the container's total energy as the sum of the potential and kinetic energy at the boundary of the Capture Sphere should exceed the potential energy in the L6 and L7 saddles. This condition allows us to determine the minimum possible velocity at the boundary of the Capture Sphere. The reverse integration method will be used as a backward integration method [19, 20] to determine a launch point.

III. Restricted three-body problem taking into account E-field

A. Key assumptions

We introduce acceptable assumptions that do not distort a principled picture of the proposed Phobos sample return mission:

1. Mass of the electrostatic container m_3 is significantly less than mass of the Phobos m_2

$$m_3 \ll m_2 \tag{1}$$

2. The Phobos' orbit is circular. Although, in reality, this orbit has a small eccentricity ($e = 0.015$). In addition, the Martian gravity perturbations will not be taken into account, as the motion of the container within 10 meters of the L1 point will be investigated.
3. The Mars-Phobos L1 libration point is fixed in the Mars-Phobos system and the L1 point location is the fixed-point relative to the moon's surface.
4. In all considered cases only in-plane motion is studied.

B. Motion equations

Consider the equations of the container planar motion in the Local-Vertical-Local-Horizontal frame Oxy within the scope of the classical restricted three-body problem [15-16]

$$\ddot{x} = \frac{\partial W}{\partial x} + n^2 x + 2n\dot{y} + \Phi \frac{x - x_{L_1}}{R^3} \tag{2}$$

$$\ddot{y} = \frac{\partial W}{\partial y} + n^2 y - 2n\dot{x} + \Phi \frac{y}{R^3} \tag{3}$$

where

$$W(x,y) = G\left(\frac{m_1}{\sqrt{(x + d\mu)^2 + y^2}} + \frac{m_2}{\sqrt{(x - d(1-\mu))^2 + y^2}}\right) \tag{4}$$

$$\mathbf{R} = \overline{M_1 M_3} - \overline{M_1 L_1} = (X, Y) \tag{5}$$

$$\mathbf{F} = \Phi \frac{\mathbf{R}}{R^3}, \qquad (\Phi = k_C q_2 q_3) \tag{6}$$

where $\mu = \dfrac{m_2}{m_1 + m_2}$, d is the distance between Mars and Phobos, x_{L_1} is the abscissa of the Phobos L1 point, m_1 is mass of Mars, m_2 is mass of Phobos, $\mathbf{F}$ is the Coulomb force as a vector, X, Y are the coordinates of the frame L_1XY (Fig. 2). In the case of absence of the electrostatic force (6) the motion equations (2) and (3) have a first integral, called the Jacobi integral [15-16]

$$J = 2G\left(\frac{m_1}{\sqrt{(x - d(1-\mu))^2 + y^2}} + \frac{m_2}{\sqrt{(x + d\mu)^2 + y^2}}\right) + n^2(x^2 + y^2) - (\dot{x}^2 + \dot{y}^2) = const, \tag{7}$$

where J is the negative doubled total energy per unit mass in the rotating Cartesian frame Oxy. The first term corresponds to the gravitational potential, the second term represents the centrifugal potential energy, and the third is the kinetic energy. The forces that act on the container are the two gravitational attractions, the centrifugal force and the Coriolis force. Since the first three can be derived from potentials and the last one is perpendicular to the trajectory, they are all conservative. Therefore, the energy conserves its constant value.

Since we study the motion of the container relative to the orbiter, which is in the L1 point, it makes sense to pass from the frame Oxy to the L1-container frame L_1XY by changing the variable (Fig. 2)

$$x = X + x_{L_1}, \qquad y = Y. \tag{8}$$

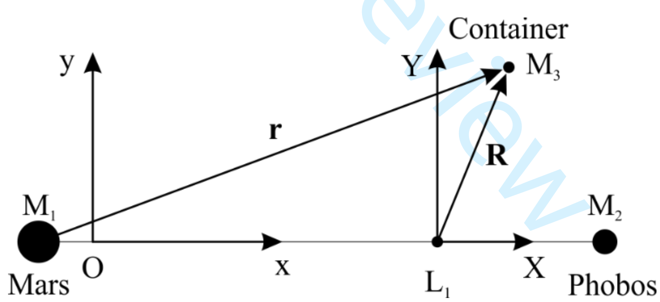

Fig. 2 The L1-container frame L_1XY

Then taking into account (8), the motion equations (2) and (3) can be rewritten as

$$\ddot{X} = \frac{\partial W_E}{\partial X} + n^2(X + x_{L_1}) + 2n\dot{Y} \tag{9}$$

$$\ddot{Y} = \frac{\partial W_E}{\partial Y} + n^2 Y - 2n\dot{X} \tag{10}$$

where

$$W_E(X,Y) = W(X,Y) + \frac{1}{m_3} W_C(X,Y) \tag{11}$$

The Coulomb electrostatic potential in Eq. (11) is as follows

$$W_C(X,Y) = -\frac{\Phi}{\sqrt{X^2+Y^2}} \tag{12}$$

Then the full potential (11) is written as

$$W_E(X,Y) = G\left(\frac{m_1}{\sqrt{(X+x_{L_1}+d\mu)^2+Y^2}} + \frac{m_2}{\sqrt{(X+x_{L_1}-d(1-\mu))^2+Y^2}}\right) - \frac{\Phi}{m_3\sqrt{X^2+Y^2}} \tag{13}$$

The derived Eqs. (9) and (10) describe the motion of a material point (in this case the container) in a moving frame L_1XY in the gravitational field of two attracting centers (Mars and Phobos) and the Coulomb field with a center in the L1 point. However, it should also be noted that the action of the electrostatic field is limited to the Debye length [12].

So, there is a modified restricted problem of three bodies with an additional potential field, in this case, an electrostatic field. Since a potential field is added to the classical three-body problem, then, obviously, Eqs. (9) and (10) should have a new Jacobi integral, which in coordinates (X,Y) is written as

$$J_E = 2G\left(\frac{m_1}{\sqrt{(X+x_{L_1}-d(1-\mu))^2+Y^2}} + \frac{m_2}{\sqrt{(X+x_{L_1}+d\mu)^2+Y^2}}\right) + n^2 \ (X+x_{L_1})^2+Y^2$$
$$-\ \dot{X}^2+\dot{Y}^2\ -\frac{2\Phi}{m_3\sqrt{X^2+Y^2}} = const \tag{14}$$

C. Effective potential, the new libration points and the Debye sphere

In terms of the new variables (X,Y), the effective potential [13] of Eqs. (9) and (10) is as follows

$$W_*(X,Y) = \frac{1}{m_3}W_C(X,Y) + \frac{n^2}{2}\ (X+x_{L_1})^2+Y^2$$
$$= \frac{n^2}{2}\ (X+x_{L_1})^2+Y^2\ + G\left(\frac{m_1}{\sqrt{(X+x_{L_1}+d\mu)^2+Y^2}} + \frac{m_2}{\sqrt{(X+x_{L_1}-d(1-\mu))^2+Y^2}}\right) - \frac{\Phi}{m_3\sqrt{X^2+Y^2}} \tag{15}$$

The new equilibrium positions, caused by the E-field, lie on the axis L_1XY (Fig. 2), are restricted by the Debye sphere and can be found as solutions to the following equation

$$\left(\frac{\partial W_*}{\partial X}\right)_{/Y=0} = 0 \tag{16}$$

The two new libration points have been determined on an axis L_1XY as an example for $m_3 = 10\,kg$, $\Phi =$ -0.4 Nm^2 (Fig. 3a)

$$L_6 = -44.053\,m, \quad L_7 = 43.976\,m \tag{17}$$

and

$\Phi =$ -0.04 Nm^2 (Fig. 3b)

$$L_6 = -20.438\,m, \quad L_7 = 20.422\,m \tag{18}$$

Note that $\Phi =$ -0.4 Nm^2 charge level represents about a 4.5kV charge level on a 1m radius object and $\Phi =$ -0.04 Nm^2 corresponds to 1.4 kV. Only the closest points L_6 and L_7 to the L1 point make sense to consider, their distance from the L1 point does not exceed the Debye length $\lambda_D = 45\,m$, as shown in Fig. 3. In addition, the higher the electrical charge level $\Phi = k_C q_2 q_3$, the further the new unstable points L_6 and L_7 are located from the point L1 (Fig. 3).

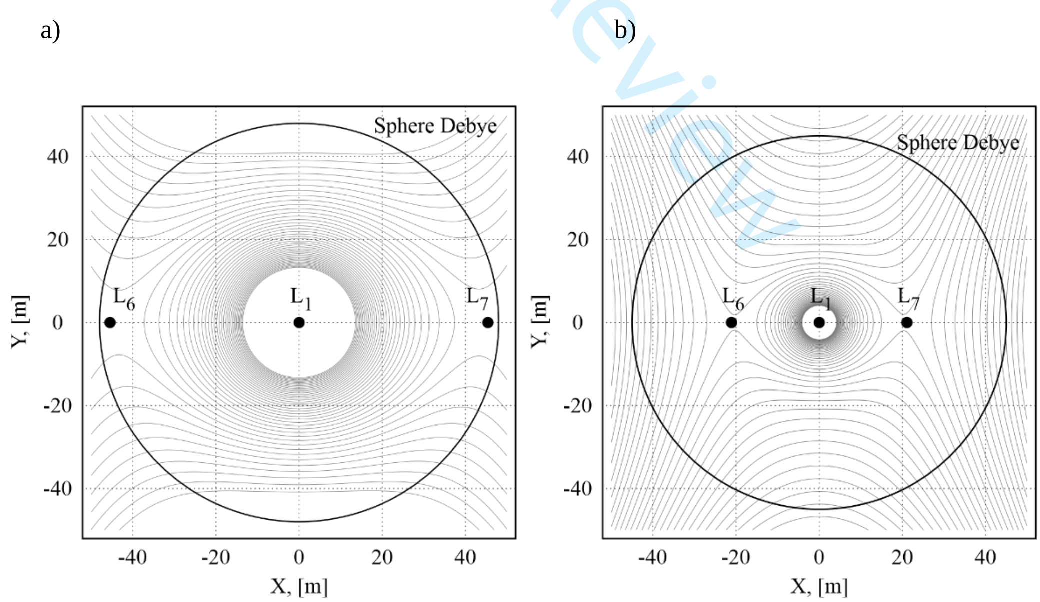

Fig. 3 Contour plot of the effective potential $W_*(X,Y)$ in the vicinity of the L1 point, when a) $\Phi =$ -0.4 $N \cdot m^2$ and b) $\Phi =$ -0.04 $N \cdot m^2$

IV. Determination the trajectory of the container

A. Determination of initial conditions of the trajectory by backward integration method

It is necessary to determine the position of the container launch point on the Phobos surface, and the launch velocity at which the container reaches the Capture Sphere boundary (Fig. 1). When entering this sphere, the container should have the lowest possible velocity, which will ensure the container's easy capture by the orbiter. Consider the system expressed by Eqs. (9) and (10). The forward integration method can be used to plot the trajectories started from any initial states. Furthermore, we are unaware in advance of what part of the state space these trajectories will lead. In this case, the backward integration method [18, 19] can be used to plot the trajectories of a new system that can be easily derived from Eqs. (9) and (10) by substituting the independent variable $t = -\tau$. At such substitution, the first derivatives change the sign to the opposite one, and the second sign derivatives do not change

$$\dot{X} = -X',\ \dot{Y} = -Y',\ \ddot{X} = X'',\ \ddot{Y} = Y'' \tag{19}$$

where $()' = \dfrac{d}{d\tau}()$. As a result, we have the new equations for the backward integration

$$X'' = \frac{\partial W_\Sigma}{\partial X} + n^2(X + x_{L_1}) - 2nY' \tag{20}$$

$$Y'' = \frac{\partial W_\Sigma}{\partial Y} + n^2 Y + 2nX' \tag{21}$$

Eqs. (20) and (21) have the same trajectories in state space as the system of Eqs. (9) and (10), but with reversed arrows on the trajectories. These equations allow us to determine the minimum possible velocity at the boundary of the Capture Sphere.

B. Determination of the end conditions of the trajectory on the Capture Sphere

The backward numerical integration starts from a point belonging to the Capture Sphere boundary. For easy container capture, its velocity at this point should be as low as possible. On the other hand, the total mechanical energy of the container should be greater than the potential energy on the outer shell of the E-Hill Sphere and, therefore, in the L6 and L7 saddle points. Only in this case, the backward integration of the container trajectory can cross the E-Sphere's outer shell from inside and leave this sphere. Likewise, the forward integration trajectory obtained can cross this boundary from the outside and reach the Capture Sphere.

Two considerations are taken into account to determine the end container velocity (or the initial velocity for the backward integration) at the Capture Sphere boundary. First, the Jacobi integral (14), which is the negative doubled total energy per unit mass, is the first integral of Eqs. (9) and (10), and, therefore, of Eqs. (20) and (21). Second, the boundary of the Capture Sphere, a priori inside the E-Sphere of Hill, can only be reached when the container's total energy is greater than the potential energy at the L6 and L7 libration points. Taking into account these two considerations and using the Jacobi integral (14), the required end velocity of the container is written as

$$V_f^2 > \frac{2Gm_1}{\sqrt{(X_f + x_{L_1} - d(1-\mu))^2 + Y_f^2}} + \frac{2Gm_2}{\sqrt{(X_f + x_{L_1} + d\mu)^2 + Y_f^2}} + n^2((X_f + x_{L_1})^2 + Y_f^2)$$

$$-\frac{2\mathrm{K}}{m_3 r_{CS}} - J_E^* \tag{22}$$

where r_{CS} is the radius of the Capture Sphere, V_f is the end velocity of the container, $(X_f = r_{CS}\cos\varphi, Y_f = r_{CS}\sin\varphi)$ are the coordinates of the end point of the container trajectory on the boundary of the Capture Sphere (Fig. 4), J_E^* is the greater value of the Jacobi integral calculated in one of the L6 and L7 libration points

$$J_E^* = \frac{2Gm_1}{\sqrt{(X_{L_{6,7}} + x_{L_1} - d(1-\mu))^2 + Y_{L_{6,7}}^2}} + \frac{2Gm_2}{\sqrt{(X_{L_{6,7}} + x_{L_1} + d\mu)^2 + Y_{L_{6,7}}^2}} + n^2((X_{L_{6,7}} + x_{L_1})^2 + Y_{L_{6,7}}^2)$$

$$-\frac{2\Phi}{m_3\sqrt{X_{L_{6,7}}^2 + Y_{L_{6,7}}^2}} \tag{23}$$

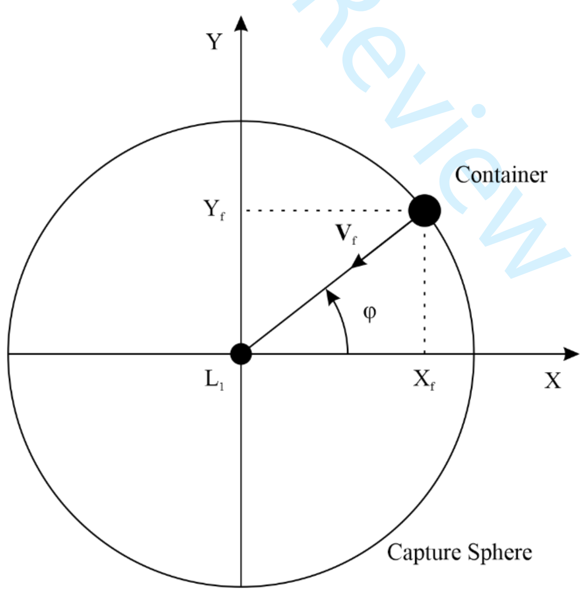

Fig. 4 The end point of the container trajectory

V. Numerical simulation

This section shows the effect of the electrostatic charge level and the Debye length on the parameters of the delivery mission of the electrostatic container from the Phobos surface to the PSR orbiter by the backward numerical simulations. In addition, the launch point of the container from the Phobos surface and the launch velocity at which the orbiter can capture the container is determined. In all cases, the container velocity $\mathbf{V}_f$ at the capture sphere boundary is directed to the L1 point, and the radius of the Capture Sphere r_{CS} is 3 m, as is accepted in [1], and the container mass is 10 kg. In the absence of accurate data on the Debye length λ_D in the L1 point, all calculations are performed for two values of this parameter, 15 m and 45 m. A Phobos planar cross-section is taken as an ellipse without taking into account the Stickney crater, which is located on the surface of Phobos directly under the L1 point. Analytically, the equation of a standard ellipse centered at the origin with are a semi-major ($2a$) and a semi-minor ($2b$) axes is

$$\frac{(X-r_h)^2}{a^2}+\frac{Y^2}{b^2}=1 \tag{24}$$

where $a=13.0\,km$ and $b=11.2\,km$ are the semi-major and the semi-minor axes, $r_h=16.812\,km$ is the distance between the L1 point and the center of this ellipse.

A series of simulations by the backward integration of Eqs. (20) and (21) is performed, changing only the φ (Fig. 4). Only the container trajectories that reach the Phobos surface are taken into consideration. The range of possible angles φ is determined $\left[\varphi_- \le \varphi \le \varphi_+\right]$. The performed simulations showed that the launch point and the launch velocity depend little on this angle. The following cases are considered:

a) $\lambda_D=45\,m$, $\Phi=k_C q_2 q_3=-0.4\,\mathrm{N}\cdot\mathrm{m}^2$ (Fig. 5).

b) $\lambda_D=45\,m$, $\Phi=k_C q_2 q_3=-0.015\,\mathrm{N}\cdot\mathrm{m}^2$ (Fig. 6a).

c) $\lambda_D=15\,m$, $\Phi=k_C q_2 q_3=-0.015\,\mathrm{N}\cdot\mathrm{m}^2$ (Fig. 6b).

Table 1 contains the following numerical simulation results for the above three cases: the launch point coordinates in the frame L_1XY (X_0,Y_0), the start and the end velocities (V_0,V_f), the start velocity angle α and the mission time T. The acceptable angular range at the Capture Sphere boundary is the same in all cases $(\varphi_-,\varphi_+)=(-1.9,\ 1.1)rad$.

Table 1 Simulation results

Case	$\Phi, \mathrm{N}\cdot\mathrm{m}^2$	$X_{L_{6,7}}, m$	λ_D, m	X_0, m	Y_0, m	$V_0, m/s$	α, rad	$V_f, m/s$	$T, hour$
a	-0.400	∓ 44.0	45	3575	1742	2.47	0.396	0.16	2.233
b	-0.015	∓ 14.7	45	3571	1722	2.47	0.398	0.03	2.779
c	-0.015	∓ 14.7	15	3571	1723	2.47	0.397	0.03	2.719

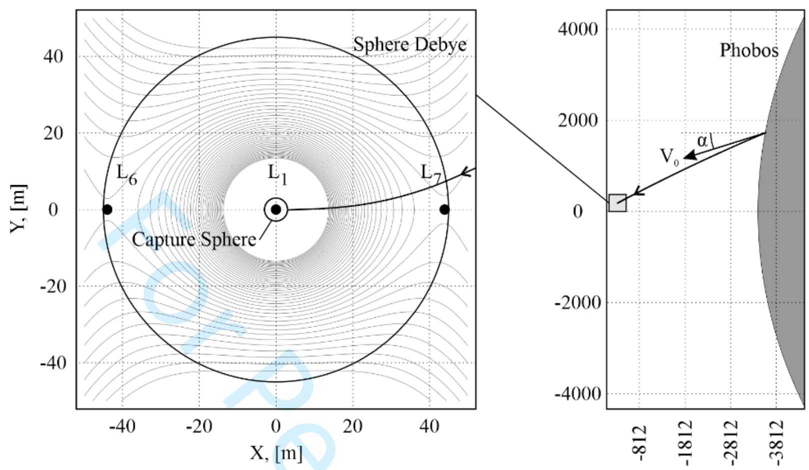

Fig. 5 The container trajectory for $\Phi = k_C q_2 q_3 = -0.4\,\mathrm{Nm}^2$ and $\lambda_D = 45\,m$

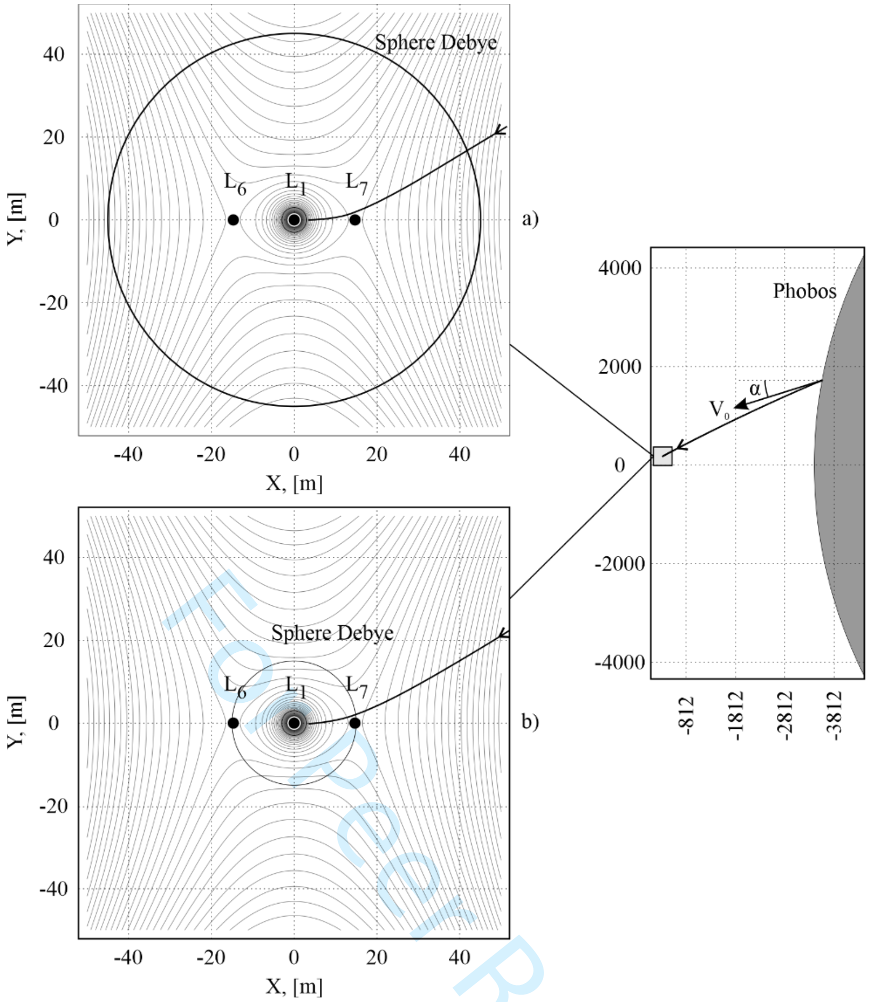

Fig. 6 The container trajectory for $\Phi = k_C q_2 q_3 = -0.015\,\mathrm{Nm}^2$ and (a) $\lambda_D = 45\,m$, (b) $\lambda_D = 15\,m$

The following comments can be made based on the simulation. First, to reach the orbiter, located at the Mars-Phobos L1 libration point, requires the container launching velocity of about 2.5 m/s, which can be easily provided by a spring pusher. Second, the lower the electric charge level $\Phi = k_C q_2 q_3$, the lower the velocity, can be at the end point of the trajectory on the Capture Sphere boundary, so at $\Phi = -0.015\,\mathrm{Nm}^2$ the velocity is only $V_f = 0.03\,m/s$. This makes it easier to capture the container via a net or magnet. Third, the Debye length has little effect on the process of capturing the container. All that matters is that the Debye length was greater than the required radius of the E-Hill Sphere. Finally, note that the mission time T depends on the electric charge level Φ , and due to Phobos' weak gravity, is more than two hours. Fig. 7 depicts that the container velocity decreases as it moves away from Phobos, and only when it reaches the Capture Sphere the velocity increases through the electrostatic force. That is enough time for the PSR orbiter to be ready to capture the container.

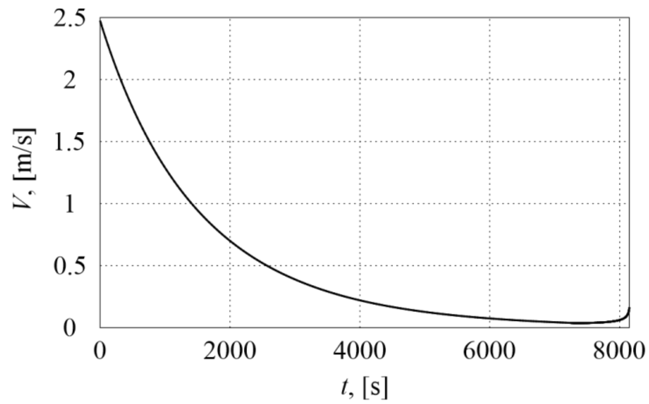

Fig. 7 The velocity profile of the container for $\Phi = k_C q_2 q_3 = -0.4\,\mathrm{Nm}^2$ and $\lambda_D = 45\,m$

VI. Conclusions

In this paper, a rationale for the mission of delivering Phobos samples to the PSR orbiter is proposed using the electrostatic container. The orbiter is actively maintaining its position at the L1 point. The attractive electrostatic field generates two unstable librations at the L6 and L7 points, located between Mars and the L1 point, and the L1 point and Phobos, respectively. From a theoretical point of view, this phenomenon generates a new case of the restricted problem of three bodies in the two gravitational fields (Mars-Phobos) and the one electrostatic field in the L1 point, when there are the six libration points. This problem was solved in the classical formulation when the motion equations and the new Jacobi integral in a simple analytical form were obtained. The container's motion was studied, and the conditions of reaching the given small neighborhood, the L1 point, were determined. The proposed mission feasibility, to deliver the electrostatic container from the Phobos surface to the PSR orbiter, is demonstrated. The influence of the electrostatic charge level and Debye length were studied on the container trajectory and the possibility of capturing the container. In addition, the possible launching points of the container from the Phobos surface and launching velocity at which the PSR orbiter could capture the container were determined by the backward numerical integration method of the motion equations. The developments were made in a general way to apply to any container by weight and electrical charge. We have shown that all stages of the proposed mission are quite feasible. Further studies of the problem will continue considering the small Phobos orbit eccentricity of $e = 0.015$ and the Martian gravity perturbations (mainly J2), as well as by investigating of the stability of container's motion in the vicinity of the L1 point. If accounting for the above perturbations, it may be necessary to follow the scheme proposed in [1] and use a small rocket to deliver the container to the Debye sphere.

Funding Sources

This study was supported by the Russian Science Foundation (Project No. 19-19-00085).

References

[1] Shibata, T., Bennett, T., and Schaub, H., "Prospects of a hybrid magnetic/electrostatic sample container retriever," *Journal of Spacecraft and Rockets*, Vol. 57, No. 3, 2020, pp. 434-445. https://doi.org/10.2514/1.A34509.

[2] Lockwood, M. K., "Introduction: Mars Science Laboratory: the next generation of Mars landers," *Journal of Spacecraft and Rockets*, Vol. 43, No. 2, 2006, pp. 257-257. https://doi.org/10.2514/1.20678.

[3] Edquist, K. T., Desai, P. N., and Schoenenberger, M., "Aerodynamics for Mars Phoenix entry capsule," *Journal of Spacecraft and Rockets,* Vol. 48, No. 5, 2006, pp. 713-726. https://doi.org/10.2514/1.46219.

[4] Gil, P. J. S. and Schwartz, J. "Simulations of Quasi-Satellite Orbits Around Phobos," Journal of Guidance, Control, and Dyrnamics, Vol. 33, No. 3, 2010, pp. 901-914. https://doi.org/10.2514/1.44434.

[5] Chen, H., Canalias, E., Hestroffer, D., and Hou, X., Effective Stability of Quasi-Satellite Orbits in the Spatial Problem for Phobos Exploration. *Journal of Guidance, Control, and Dynamics*, Published Online: 9 Aug 2020. https://doi.org/10.2514/1.G004911.

[6] Sherwood, B., "Mars Sample Return: Architecture and Mission Design," *Acta Astronautica*, Vol. 53, No. 4-10, 2003, pp. 353–364. https://doi.org/10.1016/S0094-5765(03)00153-X.

[7] O'Neil, W., and Cazaux, C., "The Mars Sample Return Project," *Acta Astronautica*, Vol. 47, No. 2-9, 2000, pp. 453–465. https://doi.org/10.1016/S0094-5765(00)00085-0.

[8] Dankanich, J., and Klein, E., "Mars Ascent Vehicle Development Status," *IEEE Aerospace Conference*, Big Sky, USA, 2012.

https://doi.org/10.1190/AERO.2012.6187295.

[9] Kempton, K., Pearson, J., Levin, E., Carroll, J., & Amzajerdian, F., "Phase 1 Study for the Phobos L1 Operational Tether Experiment (PHLOTE)," *End Report, NASA*, 2018, pp.1-91. https://ntrs.nasa.gov/search.jsp?R=20190000916.

[10] Galeev, A. A., et al., "Phobos sample return mission," *Advances in Space Research*, Vol. 17, No. 12, 1996, pp. 31-47. https://doi.org/10.1016/0273-1177(95)00757-6.

[11] Martynov, M. B., et al., "Planetary protection principles used for Phobos-Grunt mission," *Solar System Research*, Vol. 45, No. 7, 2011, pp.593-596. https://doi.org/10.1134/S0038094611070185.

[12] Hartzell, C. M., Farrell, W., and Marshall, J., "Shaking as means to detach adhered regolith for manned Phobos exploration," *Advances in Space Research*, Vol. 62. No. 8, 2018, 2213-2219. https://doi.org/10.1016/j.asr.2017.09.010.

[13] Clerc, S., Renault, H., and Losa, D., "Control of a Magnetic Capture Device for Autonomous In-orbit Rendezvous," *The International Federation of Automatic Control*, Vol. 44, No. 1, 2011, pp. 2084–2089. https://doi.org/10.3182/20110828-6-IT-1002.01499.

[14] Botta, E. M., Sharf, I., & Misra, A. K., "Contact dynamics modeling and simulation of tether nets for space-debris capture," *Journal of Guidance, Control, and Dynamics*, Vol. 40, No. 1, 2017, pp. 110-123. https://doi.org/10.2514/1.G000677.

[15] Szebehely, V., *Theory of Orbits: the Restricted Three Body Problem*, Academic Press,San Diego, 1967

[16] Schaub, H., and Junkins, J. L., *Analytical Mechanics of Space Systems*, AIAA Education Series, 2nd ed., AIAA, Reston, VA, Oct. 2009.

[17] Kluever, C.A., *Space Flight Dynamics*, John Wiley & Sons, 2018.

[18] Inampudi, R., and Schaub, H., "Orbit radial dynamic analysis of two-craft Coulomb formation at libration points," *Journal of Guidance, Control, and Dynamics*, Vol. 37, No. 2, 2014, pp. 682-691. https://doi.org/10.2514/1.55282.

[19] Holzhüter, T., "Optimal regulator for the inverted pendulum via Euler–Lagrange backward integration," *Automatica*, Vol. 40, No. 9, 2004, pp. 1613-1620. https://doi.org/10.1016/j.automatica.2004.04.012.

[20] Lee, H. K., and Han, K. W., "Analysis of nonlinear reactor systems by forward and backward integration methods," *IEEE Transactions on Nuclear Science*, Vol. 47, No. 6, 2000, pp. 2693-2698. https://doi.org/10.1109/23.901175.